Immunology
The Journal of cells, molecules, systems and technologies

British Society for immunology

IMMUNOLOGY ORIGINAL ARTICLE

Endoplasmic reticulum stress induced LOX-1$^+$ CD15$^+$ polymorphonuclear myeloid-derived suppressor cells in hepatocellular carcinoma

Jiang Nan,[1,2†] Yan-Fang Xing,[3†] Bo Hu,[4†] Jian-Xin Tang,[1,2] Hui-Min Dong,[4] Yu-Mei He,[5] Dan-Yun Ruan,[6] Qing-Jian Ye,[7] Jia-Rong Cai,[8] Xiao-Kun Ma,[6] Jie Chen,[6] Xiu-Rong Cai,[6] Ze-Xiao Lin,[6] Xiang-Yuan Wu[2,6] and Xing Li[2,6]

[1]*Department of Hepatic Surgery, The Third Affiliated Hospital of Sun Yat-sen University, Guangzhou,* [2]*Department of Liver Surgery and Guangdong Key Laboratory of Liver Disease Research, The Third Affiliated Hospital of Sun Yat-sen University, Guangzhou,* [3]*Department of Nephrology, The Third Affiliated Hospital of Guangzhou Medical University, Guangzhou,* [4]*Department of Central Laboratory, The Third Affiliated Hospital of Sun Yat-sen University, Guangzhou,* [5]*Institute of Human Virology, Zhongshan School of Medicine, Sun Yat-Sen University, Guangzhou,* [6]*Department of Medical Oncology and Guangdong Key Laboratory of Liver Disease Research, The Third Affiliated Hospital of Sun Yat-sen University, Guangzhou,* [7]*Department of Gynaecology, The Third Affiliated Hospital of Sun Yat-sen University, Guangzhou, and* [8]*Department of Urology, The Third Affiliated Hospital of Sun Yat-sen University, Guangzhou, China*

doi:10.1111/imm.12876
Received 11 April 2017; revised 3 November 2017; accepted 27 November 2017.
†These authors contributed equally to this work.
Correspondence: Xing Li, Department of Medical Oncology and Guangdong Key Laboratory of Liver Disease Research, the Third Affiliated Hospital of Sun Yat-sen University, 600 Tianhe Road, Guangzhou 510630, China. Email: lixing9@mail.sysu.edu.cn
and
Xiang-Yuan Wu, Department of Medical Oncology and Guangdong Key Laboratory of Liver Disease Research, the Third Affiliated Hospital of Sun Yat-sen University, 600

Summary

A recent study indicated that Lectin-type oxidized LDL receptor-1 (LOX-1) was a distinct surface marker for human polymorphisms myeloid-derived suppressor cells (PMN-MDSC). The present study was aimed to investigate the existence LOX-1 PMN-MDSC in hepatocellular carcinoma (HCC) patients. One hundred and twenty-seven HCC patients, 10 patients with mild active chronic hepatitis B, 10 liver cirrhosis due to hepatitis B, 10 liver dysplastic node with hepatitis B and 50 health control were included. LOX-1$^+$ CD15$^+$ PMN-MDSC were significantly elevated in HCC patients compared with healthy control and patients with benign diseases. LOX-1$^+$ CD15$^+$ PMN-MDSC in circulation were positively associated with those in HCC tissues. LOX-1$^+$ CD15$^+$ PMN-MDSCs significantly reduced proliferation and IFN-γ production of T cells with a dosage dependent manner with LOX-1$^-$ CD15$^+$ PMNs reached negative results. The suppression on T cell proliferation and IFN-γ production was reversed by ROS inhibitor and Arginase inhibitor. ROS level and activity of arginase of LOX-1 $^+$CD15$^+$ PMN were higher in LOX-1$^+$ CD15$^+$ PMN-MDSCs than LOX-1$^-$ CD15$^+$ PMNs, as well as the expression of the NADPH oxidase NOX2 and arginase I. RNA sequence revealed that LOX-1$^+$ CD15$^+$ PMN-MDSCs displayed significantly higher expression of spliced X-box -binding protein 1 (sXBP1), an endoplasmic reticulum (ER) stress marker. ER stress inducer induced LOX-1 expression and suppressive function for CD15$^+$ PMN from health donor. For HCC patients, LOX-1$^+$ CD15$^+$ PMN-MDSCs were positively related to overall survival. Above all, LOX-1$^+$ CD15$^+$ PMN-MDSC were elevated in HCC patients and suppressed T cell proliferation through ROS/Arg I pathway induced by ER stress. They presented positive association with the prognosis of HCC patients.

Keywords: endoplasmic reticulum stress; hepatocelluar carcinoma patients; lectin-type oxidized LDL receptor-1; polymorphonuclear myeloid-derived suppressor cell; prognosis.

Tianhe Road, Guangzhou 510630, China.
Email: wuxiangy@mail.sysu.edu.cn
Senior author: Xing Li and Xiang-Yuan Wu

Introduction

Myeloid-derived suppressor cells (MDSC) have been suggested to be a novel target for many malignant diseases,[1] including hepatocellular carcinoma (HCC).[2–5] However, target agents on MDSC have not displayed promising efficacy for HCC patients.[6] One of the critical reasons is the heterogeneity of MDSC testing among different centres.[2–5,7] At present, the standard method to separate MDSC is by density gradient centrifugation only in peripheral blood (PB).[7,8] This testing technology is not easily standardized between laboratories, which might be a critical cause of the heterogeneity of results in MDSC-targeted studies. Thus, a method that is more easily standardized between laboratories is needed to pave the way to the clinical usage of MDSC-targeted therapy.

Another critical issue for MDSC-targeted therapy is the shortage of specific surface markers to separate MDSC from neutrophils. A recent study indicated that lectin-type oxidized LDL receptor-1 (LOX-1) is a distinct surface marker for human MDSC, which is the first novel marker for polymorphonuclear myeloid-derived suppressor cells (PMN-MDSC).[7] Also, the LOX-1$^+$ PMN-MDSCs were tested in whole blood (WB), which made the procedure easier in practical terms to be standardized between laboratories.

In the present study we investigated the existence of LOX-1 PMN-MDSC in HCC patients, their latent mechanism and their association with clinical parameters.

Methods

Patients and healthy donors

During the period between June 2016 and September 2016, we investigated a series of 127 HCC patients before anticancer treatment, 10 patients with mild active chronic hepatitis B (alanine aminotransferase above twice the upper limit of normal without liver failure), 10 patients with liver cirrhosis due to hepatitis B and 10 patients with liver dysplastic node with hepatitis B in the Third Affiliated Hospital of Guangzhou Medical University and the Third Affiliated Hospital of Sun Yat-sen University, Guangzhou, China. The diagnosis of HCC was confirmed by pathology or the American Association for the Study of Liver Diseases radiological criteria by either computed tomography (CT) or magnetic resonance imaging (MRI). Age- and gender-matched healthy controls (n = 50) consisted of local volunteers. All patients and healthy controls were also screened for serum human immunodeficiency virus (HIV) antibody, hepatitis B surface antigen (HBsAg), hepatitis C virus (HCV) antibody, hepatitis D virus (HDV) antigen and HDV antibody. Patients and healthy controls who were positive for HIV, chronic hepatitis virus infection (except for hepatitis B virus) and other acute infections (including pneumonia, urinary tract infection, etc.) who were pregnant, patients who received systematic corticosteroids, immnunosuppressive agents or anticancer therapies and those with fever were excluded from this study. This study was approved by the Clinical Ethics Review Board of the Third Affiliated Hospital of Guangzhou Medical University and the Third Affiliated Hospital of Sun Yat-sen University. Written informed consent was obtained from all patients at the time of admission.

Peripheral blood mononuclear cells (PBMC) isolation and flow cytometric analysis

Blood samples were analysed within 6 hr after sampling. PBMCs were isolated from WB by Ficoll centrifugation. The following antihuman antibodies were purchased from eBioscience (San Diego, CA): CD11b-fluorescein isothiocyanate (FITC), human leucocyte antigen D-related-phycoerythrin (HLA-DR-PE), CD14-PE-cyanin 7 (Cy7), CD15-eFluor450, LOX-1-allophycocyanin (APC) and their corresponding isotype controls. The cell phenotypes were analysed by flow cytometry on a flow cytometric fluorescence-activated cell sorter (FACS)Aria II flow cytometer (BD Bioscience, San Jose, CA, USA), and data were analysed with FlowJo version 10.0.7 (FlowJo, Treestar, Inc., San Carlos, CA). For the flow cytometric sorting, a BD FACSAria cell sorter (BD Bioscience, San Jose, CA, USA) was used. The strategy for MDSC sorting was: LOX-1$^+$ CD15$^+$ for PMN-MDSCs and LOX-1$^-$ CD15$^+$ for PMNs from alive WB cells.

T-cell proliferation and activation assay

T-cell proliferation was determined by 5,6-carboxyfluorescein diacetate, succinimidyl ester (CFSE) dilution. Purified T cells were stained with CFSE (3 μM; Invitrogen, Carlsbad, CA), stimulated with 0·5 μg/ml 3-hr precoated anti-CD3 and 0·5 μg/ml anti-CD28 (eBioscience), and cultured alone or cocultured with autologous PMN-MDSCs/PMNs at the indicated ratios for 72 hr. The cells were then labelled for surface marker expression with CD4-PE or CD8-PE-Cy5 antibodies, and T-cell proliferation was analysed on a flow cytometer. All cultures were carried out in the presence of 20 IU/ml recombinant human interleukin (IL)-2 (PeproTech, Rocky Hill, NJ) in RPMI-1640 (Life Technologies, Gaithersburg, MD) for 72 hr at 37°. Where indicated,

0·5 mM N-hydroxyl-nor-l-arginine (nor-NOHA) (Cayman Chemicals, Chemicals, Ann Arbor, MI), an arginase I specific inhibitor, 1 mM L-arginine or 1 mM N-acetylcysteine (Sigma, Darmstadt, Germany), an reactive oxygen species (ROS) inhibitor, was added to the culture on day 0.

Measurement of intracellular ROS

ROS measurements were determined using the 2′,7′-dichlorofluorescein diacetate (DCFDA) stain. Briefly, WB were incubated with 2·5 μM DCFDA at 37° for 30 min after red blood cell lysis. Cells were then washed and resuspended in phosphate-buffered saline (PBS), stained with CD15-eFluor450 and LOX-1-APC at 4° for 30 min. ROS was analysed using flow cytometer with excitation and emission wavelengths of 490 and 520 nm, respectively, in LOX-1$^+$ CD15$^+$ cells and LOX-1$^-$ CD15$^+$ cells.

Enzyme-linked immunosorbent assay (ELISA)

Culture supernatants of the T cell and MDSC co-culture system were collected for ELISA testing. Interferon (IFN)-γ quantification in culture supernatants was determined using an ELISA following the manufacturer's instructions (DKW12-1000-09; Dakewe Bioengineering Co., Shenzhen, Guangdong).

Arginase activity assay

The arginase activity was measured in cell lysates. Briefly, cells were lysed with 0·1% Triton X-100 for 30 min, then 25 mM Tris-HCl and 10 mM $MnCl_2$ was added. The enzyme was activated by heating at 56° for 10 min. Arginine hydrolysis was performed by incubating the lysate with 0·5 M L-arginine for 120 min at 37°. After the addition of α-isonitrosopropiophenone (dissolved in 100% ethanol), the urea concentration was measured at 540 nm, followed by heating at 95° for 30 min.

Quantitative reverse transcription–polymerase chain reaction (qRT–PCR)

RNA was extracted with a multisource total RNA miniprep kit (AXYGEN Biosciences, Hangzhou, China) and qRT–PCR was performed utilizing commercially available primers (Supporting information, Table S2) and SYBR Premix Ex Taq II (Code, DRR081; Takara Biotechnology (Dalian) Co., Ltd, Dalian, China). Fluorescence for each cycle was quantitatively analysed using the ABI Prism 7000 sequence detection system (Life Technologies, Gaithersburg, MD). The results were reported as relative expression, normalized with the β-actin housekeeping gene as endogenous control and expressed in arbitrary units (primers used are shown in Supporting information, Table S1).

ChIP assay

The chromatin immunoprecipitation (ChIP) assay was performed following the instructions from Millipore (Billerica, MA). In brief, LOX-1$^+$ CD15$^+$ PMN-MDSCs were fixed with a 1% formaldehyde solution, lysed and sheared by sonication. Cell lysates were precleared with protein G-agarose and immunoprecipitated with specific antibodies or an anti-immunoglobulin (Ig)G control. Antibody–chromatin complexes were collected with protein G-agarose. The DNA in the complex was recovered and quantitated by qPCR. Ten per cent of the lysate before immunoprecipitation was used as the input control. Amplification of cyclophilin from the input was used as a loading control. For sequential ChIP assays, samples were immunoprecipitated with anti-XBP1 antibody (619502, Biolegend, San Diego, CA, USA). DNA from both rounds of ChIP assays was purified and subjected to qPCR (primers used are shown in Supporting information, Table S1).

Immunohistochemistry (IHC)

HCC tissues were sectioned at 4-μm thickness, dewaxed with xylene, rehydrated with graded ethanol and immersed in sodium citrate (pH 6·0) for antigen retrieval using a microwave. IHC was conducted according to the manufacturer's protocol [ab210059 DoubleStain IHC Kit: M&R on human tissue, diaminobenzidine (DAB) & AP/Red, abcam, Cambridge, MA] Slides were incubated in blocking reagent; rabbit [anti-LOX 1 antibody ab126538, abcam, Cambridge, MA) and mouse [anti-CD15 antibody (FUT4/815) bovine serum albumin (BSA)] and azide-free ab212396, abcam, Cambridge, MA) primary antibody mixture were used to cover the tissue and incubated. Rabbit AP polymer and mouse HRP polymer were added and incubated. DAB working solution was applied to completely cover the tissue and incubated. Then, Permanent Red working solution was added and incubated and counterstained with haematoxylin and incubated, washing between steps with PBS-T. Aqueous mounting medium was added horizontally in an oven at 40–50° for at least 30 min until the slides were thoroughly dried.

Two pathologists, who were blinded to the clinicopathological and follow-up information, evaluated IHC staining independently. Visible brown staining was considered to indicate positive staining for CD15 with red for LOX-1. Double-positive cells were counted in each mm^2.

Western blotting

Lysates from LOX-1$^+$ CD15$^+$ PMN-MDSCs and LOX-1$^-$ CD15$^+$ PMN containing 100 μg protein were incubated with 2 μg of antibodies against interested proteins (rabbit monoclonal to XBP1, ab109221, abcam; rabbit monoclonal to activating transcription factor 3 (ATF3),

ab 207434, abcam; mouse monoclonal to DDIT3, ab11419, abcam) for 18 hr at 4°, followed by incubation with protein A/G agarose for 1 hr at 4°. The immunoprecipitates were then washed with PBS and heated at 95° for 5 min, followed by centrifugation at 5000 ***g*** for 1 min. The supernatants were then subjected to Western blotting analysis. Briefly, target molecules were detected using specific primary antibodies and horseradish peroxidase (HRP)-conjugated secondary antibodies, followed by detection using an enhanced chemiluminescence (ECL) HRP chemiluminescent substrate reagent kit (Invitrogen).

RNA-sequencing data analysis

LOX-1$^+$ CD15$^+$ PMN-MDSCs and LOX-1$^-$ CD15$^+$ PMN from HCC patients were enriched by CD15b-beads and then sorted on a FACSAria cell sorter (BD Bioscience). The sorting purity was > 95%. RNA sequencing was performing using Illumina Hiseq 2500 platform (Illumina, San Diego, CA). A VAHTS total RNA-Seq library preparation kit (Vazyme Biotech Co., Ltd, China) was used for library preparation. Single-end read runs were used, with read lengths up to 50 base pairs (bp) in high output mode, 20 M total read counts. Data were aligned using RSEM version 1.2.12 software against 10-mm genome and gene-level read counts and reads per kilobase of transcript per million mapped reads (RPKM) values at gene level were estimated for ensemble transcriptome. Samples with at least 80% aligned reads were analysed. DESeq2 was used to estimate the significance between any two experimental groups. Overall changes were considered significant if they passed false discovery rate (FDR) < 5% thresholds, with an additional threshold on fold change (fold > 1·2) taken to generate the final gene set.

Patient follow-up and statistical analysis

Patients returned for follow-up appointments at least every 2 weeks during the first 6 months, and then every month thereafter until death. The follow-up duration was calculated from the first day of therapy to the day of death or to the last examination. Overall survival (OS) was the end-point, which was calculated from the first day of treatment to death.

Variables in different groups were compared using the χ^2 test (or Fisher's exact test, if indicated) and *t*-test or non-parametric Mann–Whitney *U*-tests. OS was calculated using the Kaplan–Meier method, and the differences were compared using the log-rank test. The criterion for statistical significance was set at $\alpha = 0{\cdot}05$ and all *P*-values were based on two-sided tests. For *in-vitro* experiments, statistical analyses were performed using paired *t*-tests. Correlations between different parameters were analysed using a Spearman's rank test. Statistical tests were performed using GraphPad PRISM version 5.0a and SPSS Statistics 20.0 (SPSS, Chicago, Illinois). *P* values of 0·05 were considered significant.

Results

LOX-1$^+$ CD15$^+$ PMN-MDSC expansion in HCC patients

During the period between June 2016 and September 2017, we investigated a series of HCC patients before anticancer treatment ($n = 127$), patients with mild active chronic hepatitis B ($n = 10$), liver cirrhosis due to hepatitis B ($n = 10$) and liver dysplastic node with hepatitis B ($n = 10$) in two centre hospitals. Age- and gender-matched healthy controls ($n = 50$) consisted of local volunteers. Blood samples were collected at the disease diagnosis. Peripheral blood mononuclear cells (PBMCs) were isolated from WB by Ficoll centrifugation and analysed within 6 hr after blood sampling. Circulating frequencies of PMN-MDSCs in PBMC were defined by classic markers (CD11b$^+$ CD14$^-$ HLA-DR$^{-/low}$ CD15$^+$).[9] LOX-1$^+$ CD15$^+$ PMN-MDSC were tested both in WB[7] (Fig. 1a) and PBMC (Fig. 1b). LOX-1$^+$ CD15$^+$ PMN-MDSC were significantly elevated in both WB and PBMC of HCC patients compared with healthy controls. Patients with mild active chronic hepatitis B, liver cirrhosis due to hepatitis B and liver dysplastic node with hepatitis B did not present increased levels of LOX-1$^+$ CD15$^+$ PMN-MDSC. The morphology of LOX-1$^+$ CD15$^+$ PMN-MDSC presented band-shaped nuclei with LOX-1$^-$ CD15$^+$ PMNs presented polymorphonuclear type (Fig. 1c). Notably, PBMC was used to enrich MDSC; thus, LOX-1$^+$ CD15$^+$ PMN-MDSC should be more abundant in PBMC than WB. We found that LOX-1$^+$ CD15$^+$ PMN-MDSC were much more abundant in PBMC than in WB (Fig. 1d) Then, in order to illustrate the association of LOX-1$^+$ CD15$^+$ PMN-MDSC in circulation and tumour tissues, IHC were utilized to test the LOX-1$^+$ CD15$^+$ PMN-MDSC. The density of LOX-1$^+$ CD15$^+$ PMN-MDSC in tumour tissue was positively related to that in circulation (Fig. 1e).

LOX-1$^+$ CD15$^+$ PMN-MDSCs suppressed T-cell activation

Suppressive ability to T-cell proliferation was the key characteristic of MDSC. In order to confirm the immune suppressive capacity of LOX-1$^+$ CD15$^+$ PMN-MDSCs in HCC patients, T cells, LOX-1$^+$ CD15$^+$ PMN-MDSCs and LOX-1$^-$CD15$^+$ neutrophils (PMNs) were purified from WB using flow sorting, respectively. CFSE-labelled PBMC-derived CD3$^+$ homologous T cells were stimulated with anti-CD3/anti-CD28 with the indicated ratio of LOX-1$^+$ CD15$^+$ PMN-MDSCs or LOX-1$^-$ CD15$^+$ PMN.[10] Addition of PMN-MDSCs resulted in significantly reduced proliferation of both

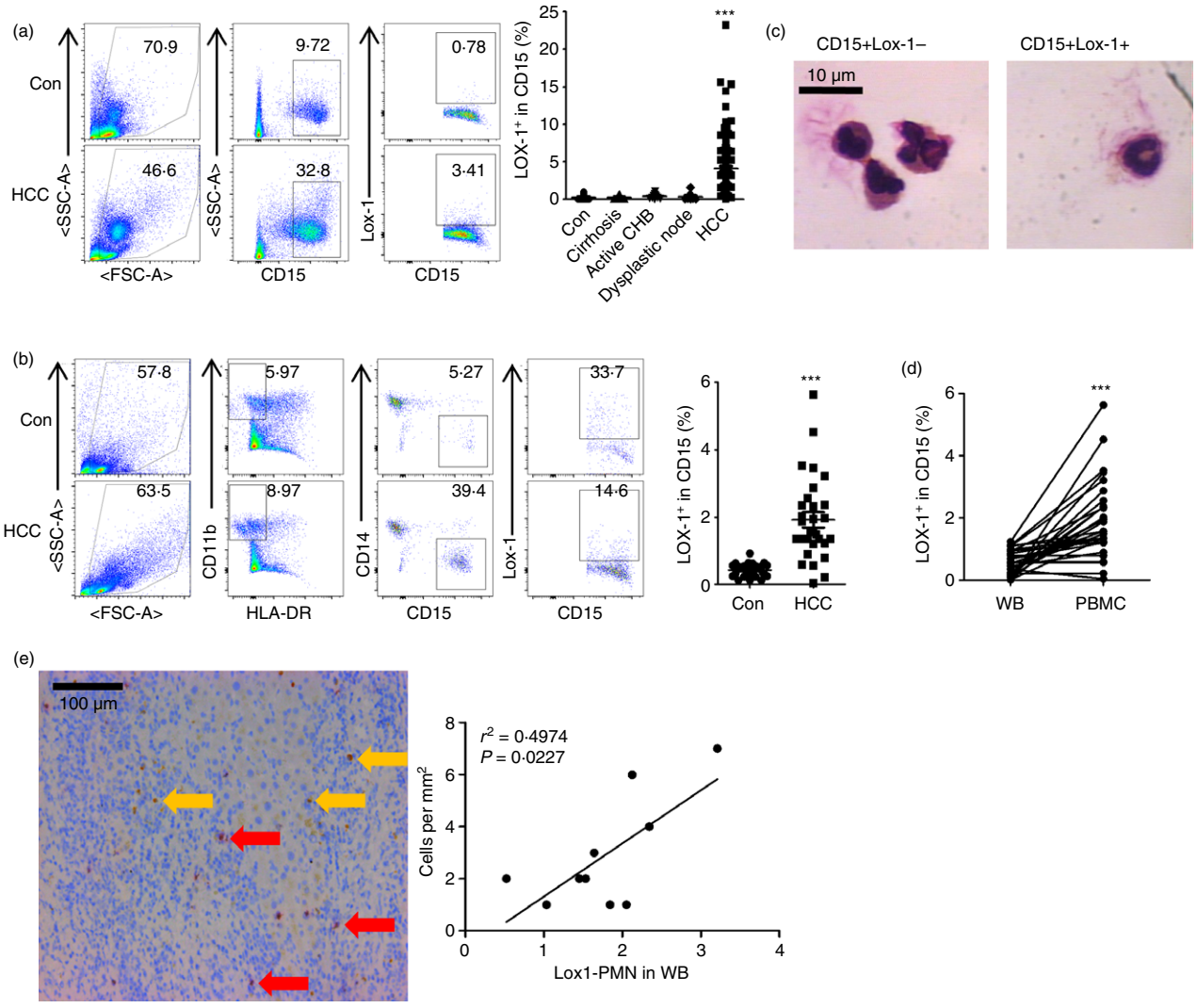

Figure 1. Expansion of lectin-type oxidized LDL receptor-1 (LOX-1)$^+$ CD15$^+$ polymorphonuclear myeloid-derived suppressor cells (PMN-MDSC) in peripheral blood mononuclear cells (PBMC) and whole blood (WB) in hepatocellular carcinoma (HCC) patients. (a) Gating strategy and statistical analysis of LOX-1$^+$ CD15$^+$ PMN-MDSCs by flow cytometry analysis in WB of HCC patients and health control. (b) Expression of LOX-1 of human leucocyte antigen D-related (HLA-DR)$^{-/low}$CD11b$^+$ CD15$^+$ CD14$^-$ PMN-MDSCs in PBMC from HCC patients and healthy controls. ***$P < 0{\cdot}001$. (c) Typical morphology of sorted LOX-1$^+$ and LOX-1$^-$ PMN from a patient with HCC. (d) the frequency of LOX-1$^+$ CD15$^+$ PMN-MDSC in the PBMC and WB from the same patient. (e) Immunohistochemistry analysis of LOX-1 (red) and CD15 (brown) expression. Brown arrow indicates LOX-1$^-$ CD15$^+$ PMN-MDSC. Red arrow indicates LOX-1$^+$ CD15$^+$ PMN-MDSC.

CD4$^+$ and CD8$^+$ T cells in a dose-dependent manner. The IFN-γ levels in the media were tested using ELISA; IFN-γ secretion decreased after administration of LOX-1$^+$ CD15$^+$ PMN-MDSCs. LOX-1$^-$ CD15$^+$ PMNs presented no suppressive function (Fig. 2).

Production of ROS and activation of arginase I were the mechanism for LOX-1$^+$ CD15$^+$ PMN-MDSC-mediated immune suppression

Based on the finding that LOX-1$^+$ CD15$^+$ PMN-MDSCs from HCC patients suppressed antigen non-specific T-cell proliferation, we further explored the underlying mechanisms controlling LOX-1$^+$ CD15$^+$ PMN-MDSC-mediated T-cell suppression. Previous reports have confirmed that arginase I or ROS were immune mediators for PMN-MDSC-mediated immune suppression.[9] Thus, arginase inhibitor nor-NOHA, L-arginine supplementation or N-acetyl-L-cysteine (NAC), a ROS inhibitor, were utilized to reverse the suppressive effects of LOX-1$^+$ CD15$^+$ PMN-MDSCs on T-cell proliferation in the coculture system.[10] As a result, the suppression of T-cell proliferation and IFN-γ production was reversed by ROS inhibitor NAC, nor-HOHA and L-arginine (Fig. 3a). We then investigated the ROS level of LOX-1$^+$ CD15$^+$ PMN by DCFDA, which indicated that the ROS levels were

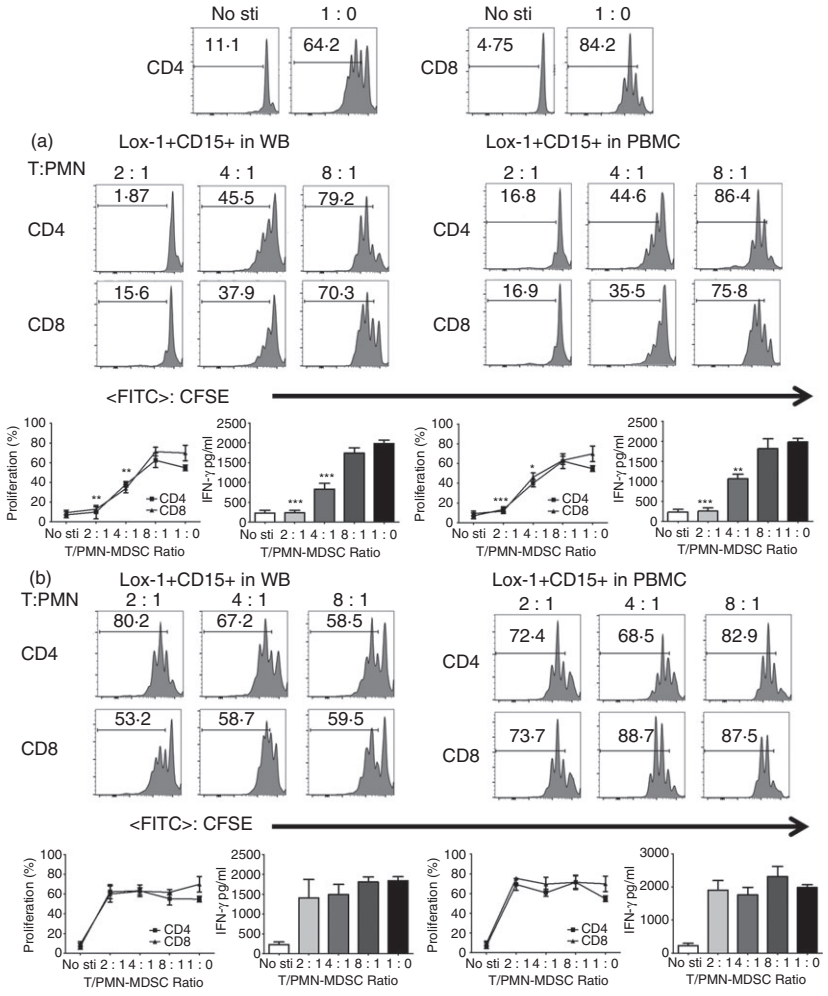

Figure 2. Lectin-type oxidized LDL receptor-1 (LOX-1)$^+$ CD15$^+$ polymorphonuclear myeloid-derived suppressor cells (PMN-MDSC) from whole blood (WB) and peripheral blood mononuclear cells (PBMC) of hepatocellular carcinoma (HCC) patients suppressed T-cell proliferation and activation. CD3$^+$ T cells from PBMC were stimulated with anti-CD3/anti-CD28, cocultured with LOX-1$^+$ CD15$^+$ PMN-MDSCs (a) or LOX-1$^-$ CD15$^+$ PMN (b) from the same donors at different ratios for 3 days, evaluated for CD4$^+$ and CD8$^+$ T cell proliferation by 5,6-carboxyfluorescein diacetate, succinimidyl ester (CFSE) labelling and interferon (IFN)-γ production in supernatants by ELISA. Down cumulative data ($n = 4$) and concentration of IFN-γ in the media ($n = 4$). $^{**}P < 0{\cdot}01$; $^{***}P < 0{\cdot}001$.

higher in HCC-related LOX-1$^+$ CD15$^+$ PMN-MDSCs than LOX-1$^-$ CD15$^+$ PMNs. Also, the mRNA levels of the nicotinamide adenine dinucleotide phosphate (NADPH) oxidase NOX2, the key protein complex responsible for ROS production in MDSCs, were higher in LOX-1$^+$ CD15$^+$ PMN-MDSC (Fig. 3b). Meanwhile, the expression of arginase I and activity of arginase were also significantly raised in HCC related LOX-1$^+$ CD15$^+$ PMN-MDSCs compared with LOX-1$^-$ CD15$^+$ PMNs (Fig. 3c).

Endoplasmic reticulum (ER) stress mediated LOX-1 expression and suppressive function of LOX-1$^+$ CD15$^+$ PMN-MDSCs

In order to test the molecular mechanism of HCC related LOX-1$^+$ CD15$^+$ PMN-MDSCs, LOX-1$^+$ CD15$^+$ PMN-MDSCs and LOX-1$^-$ CD15$^+$ PMN-MDSCs were sorted from the same patients and whole transcriptome analysis was performed using RNA-seq. A total of 124 genes were significantly different with $P < 0{\cdot}01$ and HR $> 1{\cdot}2$ or $< 0{\cdot}8$ (Fig. 4a). Cellular component analysis reveals that the intrinsic component of membrane, intracellular membrane-bound organelle, was the most changed field (Fig. 4b). Molecular function analysis revealed that binding function, including nucleic acid binding, presented the most altered genes (Fig. 4c). Combination analysis of the molecular function and cell component, the XBP1, a hallmarker for ER stress, was the most potential mechanism for HCC-related LOX-1$^+$ CD15$^+$ PMN-MDSCs. Previous studies demonstrated that PMN-MDSCs in cancer patients displayed signs of ER stress response and ER stress regulated the expression of LOX-1

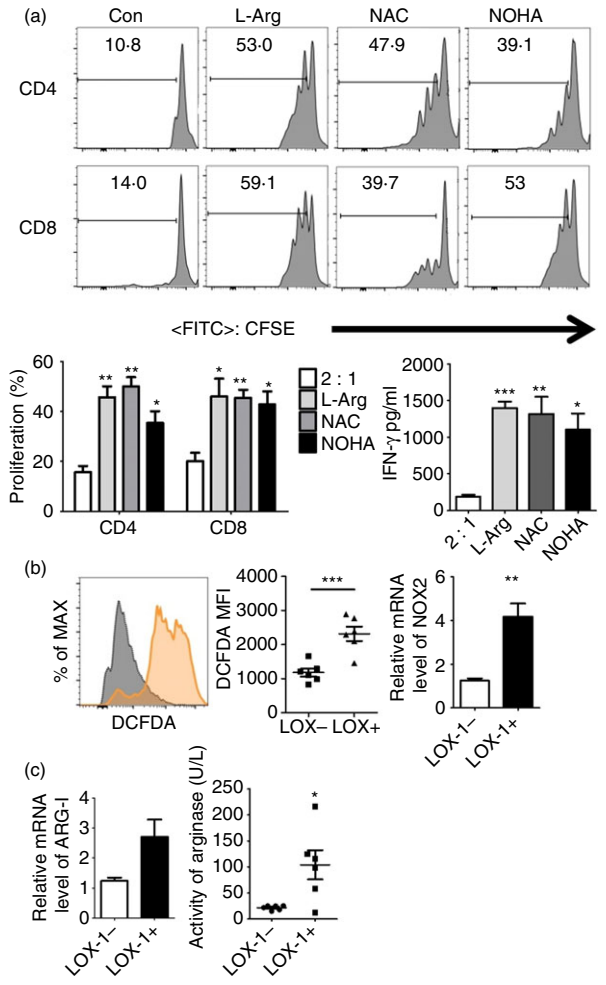

Figure 3. Lectin-type oxidized LDL receptor-1 (LOX-1)$^+$ CD15$^+$ polymorphonuclear myeloid-derived suppressor cells (PMN-MDSC) suppress functional T cells in a reactive oxygen species/arginase 1 (ROS/Arg1)-dependent manner. (a) Effect of arginase inhibitor N omega-hydroxy-L-arginine (NOHA), L-arginine supplementation or ROS inhibitor N-acetyl-L-cysteine (NAC) on LOX-1$^+$ CD15$^+$ PMN-MDSC function. T cells from end stage renal disease (ESRD) patients were stimulated with anti-CD3/anti-CD28, cocultured with LOX-1$^+$ CD15$^+$ PMN-MDSCs from whole blood at a 2 : 1 ratio with treatments as indicated, evaluated for T cell proliferation by CFSE labelling and IFN-γ production in supernatants by enzyme-linked immunosorbent assay (ELISA). Representative flow cytometry data, cumulative data ($n = 3$) and concentration of IFN-γ in the media ($n = 3$). (b) ROS level illustrated by 2′,7′-dichlorofluorescein diacetate (DCFDA) and NOX2 expression in LOX-1$^+$ CD15$^+$ PMN-MDSCs and LOX-1$^-$ CD15$^+$ PMN. Right: representative flow cytometry data. Middle: cumulative data ($n = 6$). Left: NOX2 expression. (c) Expression of Arg1 and arginase activity in LOX-1$^+$ CD15$^+$ PMN-MDSCs and LOX-1$^-$ CD15$^+$ PMN. ($n = 6$). *$P < 0{\cdot}05$; **$P < 0{\cdot}01$; ***$P < 0{\cdot}001$. [Colour figure can be viewed at wileyonlinelibrary.com]

in PMNs.[1,7] We then tested the expression of genes associated with ER stress in LOX-1$^+$ and LOX-1$^-$ PMNs. LOX-1$^+$ CD15$^+$ PMN-MDSCs displayed a significantly higher expression of spliced X-box-binding protein 1 (sXBP1) than LOX-1- PMN, confirmed by qRT–PCR and Western blot (Fig. 4d,e). Meanwhile, the expression of ATF3 and CCAAT/enhancer binding protein (CHOP) was also higher in LOX-1$^+$ PMN-MDSC tested by qRT–PCR with negative Western blot tests (Fig. 4d,e). Furthermore, we utilized ER stress inducer thapsigargin (THG) to induce the expression of LOX-1 and suppressive function in CD15$^+$ PMN from healthy donors with or without the inhibitor of XBP1, B-I09. As a result, THG-induced LOX-1 expression among CD15$^+$ PMN and THG-induced LOX-1$^+$ CD15$^+$ PMN-MDSCs presented a suppressive capability to T-cell proliferation. The efficacy of THG was abrogated by B-I09 (Fig. 5a). In order to investigate whether XBP1 regulated the promoter of LOX-1, we found the potential binding site of XBP1 in the LOX-1 promoter region (Fig. 5b). However, ChIP analysis revealed that XBP1 does not bind to the LOX-1 promoter (Fig. 5c). Tumour-conditioned media of HCC cell lines (Hu7, HepG2, 97L) and serum of HCC patients with increased LOX-1$^+$ CD15$^+$ PMN-MDSCs were used to induce LOX-1 and XBP1 expression in CD15$^+$ PMN from healthy donors. However, HCC tumour cells (TCM) and HCC serum did not increase the LOX-1 and XBP1 expression significantly, compared with controls (Fig. 5d). Above all, ER stress mediated LOX-1 expression and the suppressive function of LOX-1$^+$ CD15$^+$ PMN-MDSCs.

LOX-1$^+$ CD15$^+$ PMN-MDSC positively associated prognosis of HCC patients

According to the above results, elevated LOX-1$^+$ CD15$^+$ PMN-MDSCs potentially induced immune tolerance to tumour cells in HCC patients. We then investigated the clinical association of LOX-1$^+$ CD15$^+$ PMN-MDSCs with clinical parameters and the most widely acknowledged prognostic system, Cancer of the Liver Italian Program (CLIP) score,[11–13] for HCC patients. LOX-1$^+$ CD15$^+$ PMN-MDSCs associated with CLIP score, Child–Pugh score, PT%, Eastern Cooperative Oncology Group performance status (ECOG PS), tumour T stage, portal vein thrombosis, lymph node metastasis (Fig. 6a and Supporting information, Table S2). Patients were then divided into two parts according to LOX-1$^+$ CD15$^+$ PMN-MDSCs level. Patients with low levels of LOX-1$^+$ CD15$^+$ PMN-MDSCs presented better overall survival (Fig. 6b).

Discussion

MDSC has been confirmed to be a critical mediator for immune tolerance to multiple malignances and presents promising clinical usage by basic researches and clinical investigations.[9,14–16] Many drugs were found to eliminate

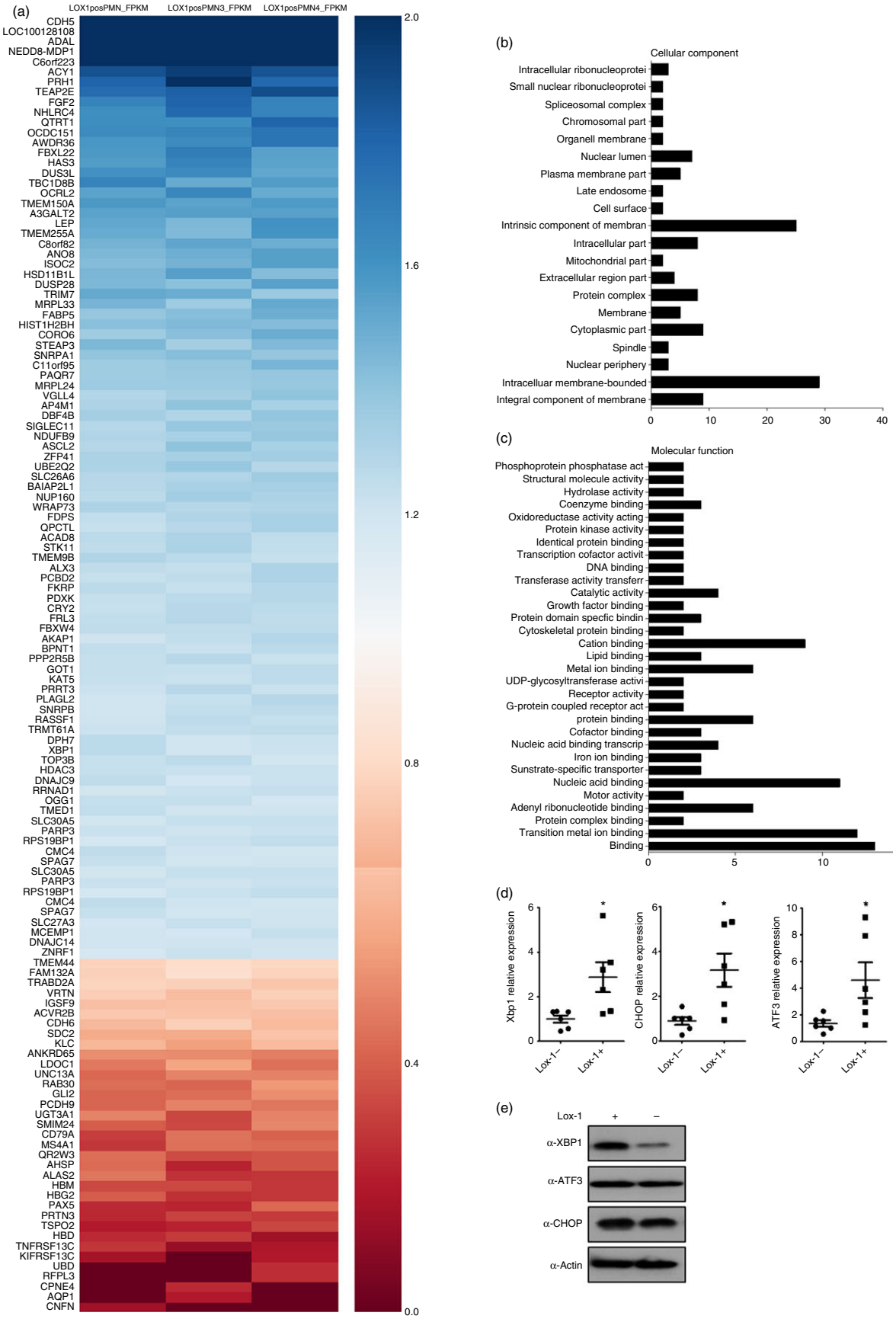
(a)
LOX1posPMN_FPKM
LOX1posPMN3_FPKM
LOX1posPMN4_FPKM
2.0
1.6
1.2
0.8
0.4
0.0
(b)
Cellular component
Intracellular ribonucleoprotei
Small nuclear ribonucleoprotei
Spliceosomal complex
Chromosomal part
Organell membrane
Nuclear lumen
Plasma membrane part
Late endosome
Cell surface
Intrinsic component of membran
Intracellular part
Mitochondrial part
Extracellular region part
Protein complex
Membrane
Cytoplasmic part
Spindle
Nuclear periphery
Intracellular membrane-bounded
Integral component of membrane
0
10
20
30
40
(c)
Molecular function
Phosphoprotein phosphatase act
Structural molecule activity
Hydrolase activity
Coenzyme binding
Oxidoreductase activity acting
Protein kinase activity
Identical protein binding
Transcription cofactor activit
DNA binding
Transferase activity transferr
Catalytic activity
Growth factor binding
Protein domain specfic bindin
Cytoskeletal protein binding
Cation binding
Lipid binding
Metal ion binding
UDP-glycosyltransferase activi
Receptor activity
G-protein coupled receptor act
protein binding
Cofactor binding
Nucleic acid binding transcrip
Iron ion binding
Sunstrate-specific transporter
Nucleic acid binding
Motor activity
Adenyl ribonucleotide binding
Protein complex binding
Transition metal ion binding
Binding
0
5
10
(d)
Xbp1 relative expression
CHOP relative expression
ATF3 relative expression
Lox-1–
Lox-1+
(e)
Lox-1
+
–
α-XBP1
α-ATF3
α-CHOP
α-Actin

Figure 4. Endoplasmic reticulum stress (ER) stress and clinical significance of lectin-type oxidized LDL receptor-1 (LOX-1)$^+$ CD15$^+$ polymorphonuclear myeloid-derived suppressor cells (PMN-MDSC) in hepatocellular carcinoma (HCC) patients. (a) Hierarchical clustering of samples based on the expression levels of genes differentially expressed between LOX-1$^+$ and LOX-1$^-$ PMN in HCC patients. (b) Cell components analysis of different genes expressed. (c) Molecular function of different genes expressed. (d) Expression of X-box–binding protein 1 (XBP1), CCAAT/enhancer binding protein (CHOP) and activating transcription factor 3 (ATF3) in LOX-1$^+$ CD15$^+$ PMN-MDSCs and LOX-1$^-$ CD15$^+$ PMN by quantitative reverse transcription–polymerase chain reaction (qRT-PCR). (n = 6). (e) Expression of XBP1, CHOP and ATF3 in LOX-1$^+$ CD15$^+$ PMN-MDSCs and LOX-1$^-$ CD15$^+$ PMN by Western blot.

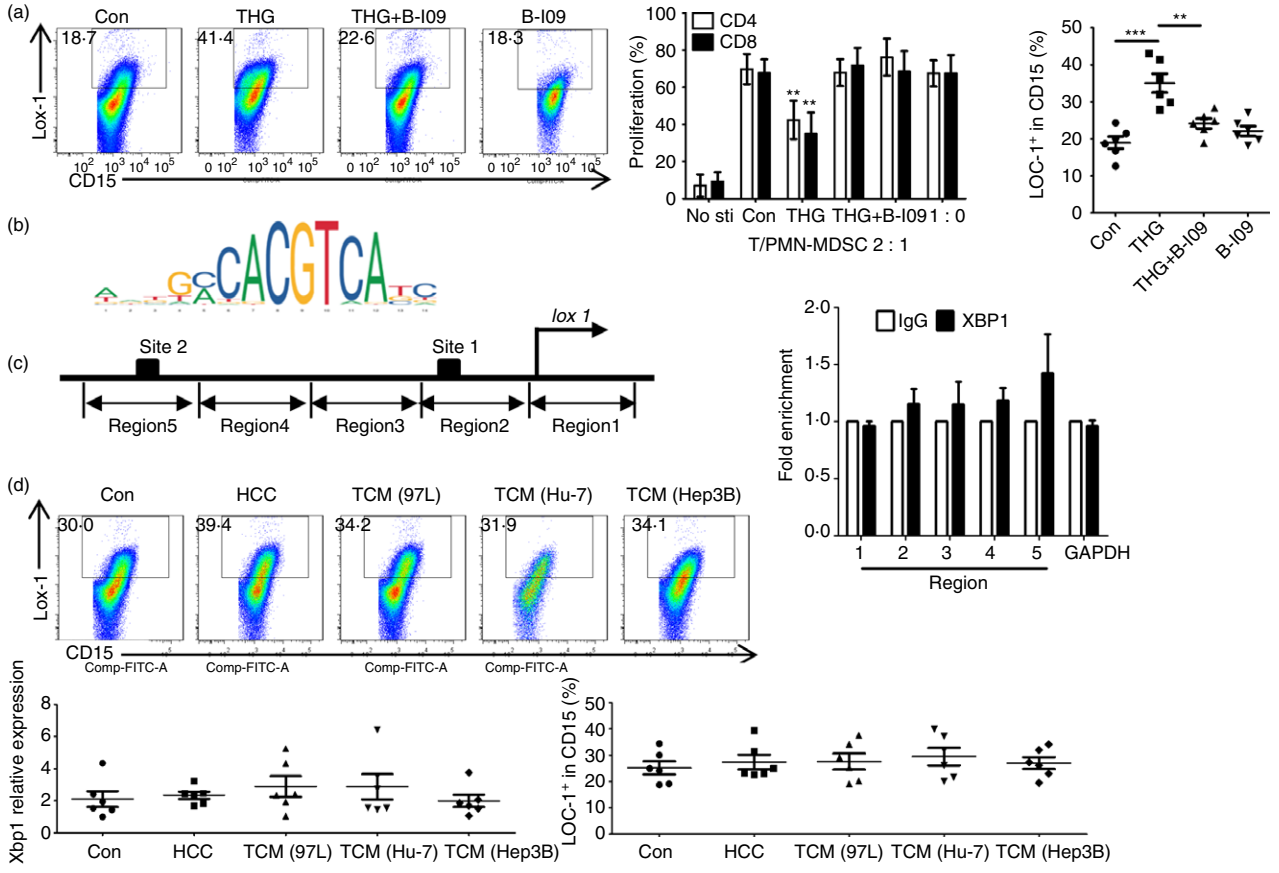

Figure 5. Endoplasmic reticulum stress (ER) stress induced lectin-type oxidized LDL receptor-1 (LOX-1) expression and suppressive function of LOX-1-CD15$^+$ polymorphonuclear cells (PMN). (a) Percentage and suppression to T cell proliferation of LOX-1$^+$ CD15$^+$ PMN-myeloid-derived suppressor cells (MDSC) derived from CD15$^+$ PMN isolated from six healthy donors and treated with 1 mM thapsigargin (THG) with or without 20 mM B-I09. (b) X-box–binding protein 1 (XBP1) binding sites in the origin of light-strand replication (OLR) promoter. (c) Chromatin immunoprecipitation (ChIP) assays were performed with LOX-1$^+$ CD15$^+$ PMN-MDSC with antibodies against XBP1 or with an immunoglobulin (Ig)G control. Recruitment of XBP1 to the LOX-1 promoter was determined by qPCR in eluted DNA. Data were normalized to the input DNA and are presented as fold increases over the values obtained with IgG. (d) Percentage of LOX-1$^+$ CD15$^+$ PMN-MDSC derived from CD15$^+$ PMN isolated from six healthy donors treated with serum from hepatocellular carcinoma (HCC) patients with increased LOX-1$^+$ CD15$^+$ PMN-MDSC and conditioned medium from HCC tumour cells (TCM) was used at 20% (v/v) concentration. [Colour figure can be viewed at wileyonlinelibrary.com]

MDSC in tumour efficiently,[6,17] which made MDSC targeted therapy practical for clinical trials. However, there has been no successful MDSC-targeted therapy since MDSC was first nominated in 2007.[6,18] One of the critical causes was the issue of testing MDSC by density gradient centrifugation, which was not a technique that was standardized easily by different laboratory.[7] Density gradient centrifugation needs strict controls on time, temperature, Ficoll density and other steps.[8] Different protocols between laboratories caused heterogenicity of the results. Thus, it is necessary to develop a method that is easily standardized. Lox-1$^+$ was the first specific marker for human PMN-MDSC in lung cancer and head and neck cancer patients.[7] PMN-MDSC is the major subtype of MDSC, which means that PMN-MDSC can be tested in WB by flow cytometry. Flow cytometry testing is a potential diagnostic technique which is used in multiple diseases, especially leukaemia. Testing Lox-1$^+$ CD15$^+$ PMN-

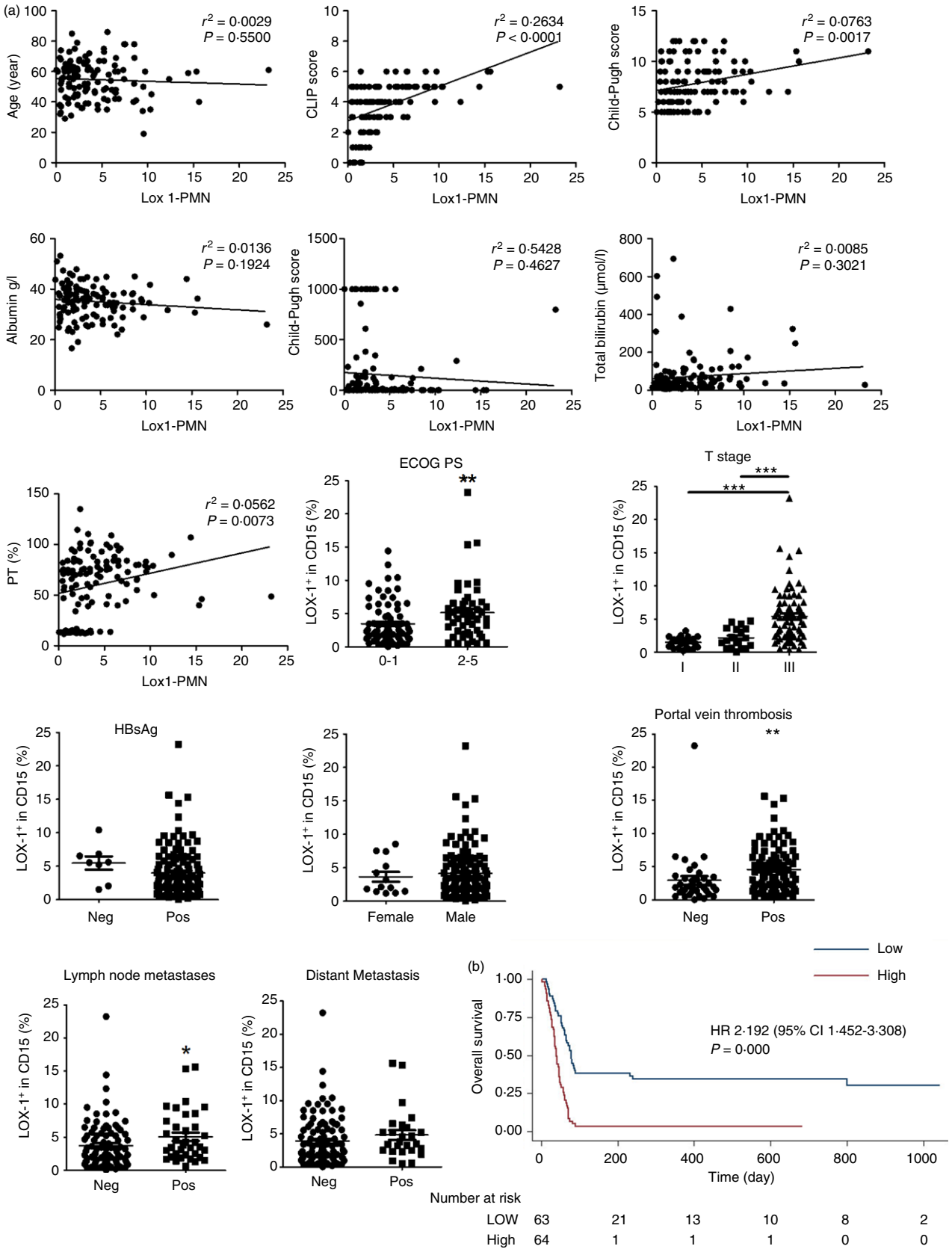
(a)
Age (year)
Lox 1-PMN
r² = 0·0029
P = 0·5500
CLIP score
Lox1-PMN
r² = 0·2634
P < 0·0001
Child-Pugh score
Lox1-PMN
r² = 0·0763
P = 0·0017
Albumin g/l
Lox1-PMN
r² = 0·0136
P = 0·1924
Child-Pugh score
Lox1-PMN
r² = 0·5428
P = 0·4627
Total bilirubin (μmol/l)
Lox1-PMN
r² = 0·0085
P = 0·3021
PT (%)
Lox1-PMN
r² = 0·0562
P = 0·0073
ECOG PS
LOX-1+ in CD15 (%)
0-1
2-5
**
T stage
LOX-1+ in CD15 (%)
I
II
III
***
***
HBsAg
LOX-1+ in CD15 (%)
Neg
Pos
LOX-1+ in CD15 (%)
Female
Male
Portal vein thrombosis
LOX-1+ in CD15 (%)
Neg
Pos
**
Lymph node metastases
LOX-1+ in CD15 (%)
Neg
Pos
*
Distant Metastasis
LOX-1+ in CD15 (%)
Neg
Pos
(b)
Low
High
Overall survival
HR 2·192 (95% CI 1·452-3·308)
P = 0·000
Time (day)
Number at risk
LOW 63 21 13 10 8 2
High 64 1 1 1 0 0

Figure 6. Prognostic value of lectin-type oxidized LDL receptor-1 (LOX-1)$^+$ CD15$^+$ polymorphonuclear myeloid-derived suppressor cells (PMN-MDSC) in hepatocellular carcinoma (HCC) patients. (a) Association between LOX-1$^+$ CD15$^+$ PMN-MDSC and clinical parameters by linear regression. (b) Kaplan–Meier survival curves are shown for overall survival in low and high LOX-1$^+$ CD15$^+$ PMN-MDSC level HCC patients. Hazard ratios (HRs) were calculated using the unadjusted Cox proportional hazards model. *P*-values were calculated using the unadjusted log-rank test; 95% CI indicates 95% confidence interval. [Colour figure can be viewed at wileyonlinelibrary.com]

MDSC by flow cytometry makes MDSC testing at the diagnostic level a near-future possibility. The present study was aimed to determine the existence and clinical usage of LOX-1$^+$ CD15$^+$ PMN-MDSC in HCC patients.

This study found that LOX-1$^+$ was the specific marker for HCC-related MDSC. LOX-1$^+$ CD15$^+$ PMN-MDSCs were elevated significantly in HCC patients and presented strong suppressive function. LOX-1$^-$ CD15$^+$ PMN was not suppressive, which indicated that the traditional definition for PMN-MDSCs (HLA-DR$^{-/low}$CD15$^+$ CD14$^-$CD11b$^+$)[9] was not accurate and contained a great number of PMNs. Also, LOX-1$^+$ CD15$^+$ PMN-MDSC were more abundant in PBMC, which indicated that LOX-1$^+$ CD15$^+$ PMN-MDSC were the real part of MDSC in HLA-DR$^{-/low}$CD15$^+$ CD14$^-$CD11b$^+$ PMN-MDSCs. More importantly, LOX-1$^+$ CD15$^+$ PMN-MDSC levels were positively related to prognosis and major prognostic factors. The clinical significance of LOX-1$^+$ CD15$^+$ PMN-MDSC makes it a potential target for immune therapy.

ER stress was reported to be the feature of MDSC,[1,7] especially for LOX-1$^+$ CD15$^+$ PMN-MDSC. In the present study, we found that LOX-1$^+$ CD15$^+$ PMN-MDSC in HCC patients presented a high level of ER stress. The bioactivator of PMN-MDSC, arginase 1 and ROS, could be the result of ER stress. These results suggest that ER stress might be the key regulator for PMN-MDSC. However, it is not clear that what caused ER stress in myeloid cell and how ER stress transfers normal myeloid cells into MDSC.[1] Tumour induced ER stress in myeloid cells by remote control, as myeloid cells distant from the tumour (PBMC) present ER stress. However, TCM and serum from HCC patients failed to induce LOX-1$^+$ CD15$^+$ PMN-MDSC and ER stress in CD15$^+$ cells from healthy donors. The latent mechanism deserves further investigation. The entire map of the ER stress pathway in LOX-1$^+$ CD15$^+$ PMN-MDSC needs further studies.

M-MDSC, HLA-DR$^{-/low}$CD15$^-$CD14$^+$ CD11b$^+$ cell in PBMC, is the other subtype of MDSC[16,17] which could not be tested directly in WB. Future studies are needed to find an easier way to test them directly in WB. Also, the sample size of the present study was not large enough to gain a reliable association between the MDSC level and prognosis. Thus, we tested the relation between LOX-1$^+$ CD15$^+$ PMN-MDSC and prognosis. Patients with high levels of LOX-1$^+$ CD15$^+$ PMN-MDSC presented a decreased OS and LOX-1$^+$ CD15$^+$ PMN-MDSC positively associated with multiple strong prognostic factors. Thus, prospective studies and clinical trials targeted on LOX-1$^+$ CD15$^+$ PMN-MDSC deserve further investigation.

In summary, the present study identified LOX-1$^+$ CD15$^+$ PMN-MDSC in HCC patients. LOX-1$^+$ CD15$^+$ PMN-MDSC suppressed T-cell proliferation through the ROS/Arg 1 pathway with ER stress as a potential feature. LOX-1$^+$ CD15$^+$ PMN-MDSC presented a positive association with the prognosis of HCC patients, which made testing LOX-1$^+$ CD15$^+$ PMN-MDSC in WB a practical technology for clinical trials targeted on MDSC.

Acknowledgements

This study was supported by National Natural Science Foundation of China (31600710, 81572368 and 81700645), the Natural Science Foundation of Guangdong (no. 2016A030313278, 2017A030313537 and 2016A030313302), Guangzhou science and technology plan (201709010030) and the Scientific Research Project of Guangzhou Municipal Universities (1201630019).

Disclosure

No conflicts of interest declared.

References

1 Condamine T, Kumar V, Ramachandran IR, Youn JI, Celis E, Finnberg N *et al.* ER stress regulates myeloid-derived suppressor cell fate through TRAIL-R-mediated apoptosis. *J Clin Invest* 2014; **124**:2626–39.

2 Hu CE, Gan J, Zhang RD, Cheng YR, Huang GJ. Up-regulated myeloid-derived suppressor cell contributes to hepatocellular carcinoma development by impairing dendritic cell function. *Scand J Gastroenterol* 2011; **46**:156–64.

3 Lacotte S, Slits F, Orci LA, Meyer J, Oldani G, Delaune V *et al.* Impact of myeloid-derived suppressor cell on Kupffer cells from mouse livers with hepatocellular carcinoma. *Oncoimmunology* 2016; **5**:e1234565.

4 Chiu DK, Xu IM, Lai RK, Tse AP, Wei LL, Koh HY *et al.* Hypoxia induces myeloid-derived suppressor cell recruitment to hepatocellular carcinoma through chemokine (C-C motif) ligand 26. *Hepatology* 2016; **64**:797–813.

5 Kalathil S, Lugade AA, Miller A, Iyer R, Thanavala Y. Higher frequencies of GARP(+) CTLA-4(+)Foxp3(+) T regulatory cells and myeloid-derived suppressor cells in hepatocellular carcinoma patients are associated with impaired T-cell functionality. *Cancer Res* 2013; **73**:2435–44.

6 Kumar V, Cheng P, Condamine T, Mony S, Languino LR, McCaffrey JC *et al.* CD45 phosphatase inhibits STAT3 transcription factor activity in myeloid cells and promotes tumor-associated macrophage differentiation. *Immunity* 2016; **44**:303–15.

7 Condamine T, Dominguez GA, Youn J-I, Kossenkov AV, Mony S, Alicea-Torres K *et al.* Lectin-type oxidized LDL receptor-1 distinguishes population of human polymorphonuclear myeloid-derived suppressor cells in cancer patients. *Science Immunol* 2016; **1**:pii: aaf8943.

8 Grutzner E, Stirner R, Arenz L, Athanasoulia AP, Schrodl K, Berking C *et al.* Kinetics of human myeloid-derived suppressor cells after blood draw. *J Transl Med* 2016; **14**:2.

9 Bronte V, Brandau S, Chen SH, Colombo MP, Frey AB, Greten TF *et al.* Recommendations for myeloid-derived suppressor cell nomenclature and characterization standards. *Nat Commun* 2016; **7**:12150.
10 Xing YF, Cai RM, Lin Q, Ye QJ, Ren JH, Yin LH *et al.* Expansion of polymorphonuclear myeloid-derived suppressor cells in patients with end-stage renal disease may lead to infectious complications. *Kidney Int* 2017; **91**:1236–42.
11 Lin ZH, Li X, Hong YF, Ma XK, Wu DH, Huang M *et al.* Alanine aminotransferase to hemoglobin ratio is an indicator for disease progression for hepatocellular carcinoma patients receiving transcatheter arterial chemoembolization. *Tumour Biol* 2016; **37**:2951–9.
12 Li X, Chen ZH, Xing YF, Wang TT, Wu DH, Wen JY *et al.* Platelet-to-lymphocyte ratio acts as a prognostic factor for patients with advanced hepatocellular carcinoma. *Tumour Biol* 2015; **36**:2263–9.
13 Li X, Chen ZH, Ma XK, Chen J, Wu DH, Lin Q *et al.* Neutrophil-to-lymphocyte ratio acts as a prognostic factor for patients with advanced hepatocellular carcinoma. *Tumour Biol* 2014; **35**:11057–63.
14 Koehn BH, Blazar BR. Role of myeloid-derived suppressor cells in allogeneic hematopoietic cell transplantation. *J Leukoc Biol* 2017; **102**:335–41.
15 Condamine T, Gabrilovich DI. Molecular mechanisms regulating myeloid-derived suppressor cell differentiation and function. *Trends Immunol* 2011; **32**:19–25.
16 Netherby CS, Abrams SI. Mechanisms overseeing myeloid-derived suppressor cell production in neoplastic disease. *Cancer Immunol Immunother* 2017; **66**:989–96.
17 Talmadge JE, Gabrilovich DI. History of myeloid-derived suppressor cells. *Nat Rev Cancer* 2013; **13**:739–52.
18 Gabrilovich DI, Bronte V, Chen SH, Colombo MP, Ochoa A, Ostrand-Rosenberg S *et al.* The terminology issue for myeloid-derived suppressor cells. *Cancer Res* 2007; **67**:425; author reply 6.

Supporting Information

Additional Supporting Information may be found in the online version of this article:

Table S1. Primers used.

Table S2. Baseline demographic and clinical characteristics of hepatocellular carcinoma patients with high or low LOX-1$^+$CD15$^+$ PMN-MDSCs in circulation.